archives
of thermodynamics
Vol. **44**(2023), No. 2, 159–175
DOI: 10.24425/ather.2023.146563

Numerical analysis of the heating of a die for the extrusion of aluminium alloy profiles in terms of thermochemical treatment

DAMIAN JOACHIMIAK*
WOJCIECH JUDT
MAGDA JOACHIMIAK

Poznan University of Technology, Institute of Thermal Engineering,
Piotrowo 3a, 60-965, Poznan, Poland

Abstract Thermochemical treatment processes are used to produce a surface layer of the workpiece with improved mechanical properties. One of the important parameters during the gas nitriding processes is the temperature of the surface. In thermochemical treatment processes, there is a problem in precisely determining the surface temperature of heat-treated massive components with complex geometries. This paper presents a simulation of the heating process of a die used to extrude aluminium profiles. The maximum temperature differences calculated in the die volume, on the surface and at the most mechanically stressed edge during the extrusion of the aluminum profiles were analysed. The heating of the die was simulated using commercial transient thermal analysis software. The numerical calculations of the die assumed a boundary condition in the form of the heat transfer coefficient obtained from experimental studies in a thermochemical treatment furnace and the solution of the nonstationary and non-linear inverse problem for the heat conduction equation in the cylinder. The die heating analysis was performed for various heating rates and fan settings. Major differences in the surface temperature and in the volume of the heated die were obtained. Possible ways to improve the productivity and control of thermochemical treatment processes were identified. The paper investigates the heating of a die, which is a massive component with complex geometry. This paper indicates a new way to develop methods for the control of thermochemical processing of massive components with complex geometries.

Keywords: Temperature distribution in a solid component; Extrusion die for aluminium profiles; Gas nitriding; Direct and inverse problem for the heat conduction equation

*Corresponding Author. Email: damian.joachimiak@put.poznan.pl

Nomenclature

c	–	specific heat, J/(kgK)
h	–	heat transfer coefficient, W/(m^{2}K)
k	–	thermal conductivity, W/(mK)
P1	–	heating process (heating rate 5 K/min, fan speed 50%)
P2	–	heating process (heating rate 5 K/min, fan speed 100%)
P3	–	heating process (heating rate 10 K/min, fan speed 50%)
T	–	temperature, K
t	–	time, s
ρ	–	density, kg/m^3

Subscripts

A	–	area
b	–	boundary
e	–	edge
g	–	gas
max	–	maximum value
min	–	minimum value
V	–	volume

1 Introduction

Aluminium hot extrusion dies are exposed to thermal and mechanical loads [1]. These profiles are created by extruding aluminium through a die at a temperature of 723 K to 772 K and at a speed of 5 to 100 m/min [1]. The complex character of the extrusion process is the reason for the problems in designing a long-life die [2]. The hard working conditions of the dies cause them to fail very often. Production of dies with a long operational life reduces the cost of the extrusion of aluminium profiles. So far, there has been analysis on tooling impact of the lifetime during hot metal forming on the efficiency and the quality of the process [3]. The damage to the dies was studied in a sample of 616 cases. Analysis of die damage is the basis for reducing the cost intensity of aluminium extrusion processes [3]. In addition to the working conditions, the shape of the die also influences the durability of the die [4], the steel grade of which it is made, and the heat and thermochemical treatment of the die [1, 5].

In the paper [6] a numerical simulation of the heat treatment of the die used in the extrusion processes is presented. In [7] the die hardening procedure for Alvar 14 steel (DIN 56 NiCrMoV7) was analysed for aluminium extrusion in vacuum furnaces. The study of the solid disc-shaped die involved experiment and numerical simulations. The values of the convective

and radiation heat transfer coefficient and Biot number were obtained. The obtained temperature gradients showed that higher heating rates could be used, which reduces the time and cost of the quenching. The simulation of heat flow in a heat treatment or thermochemical furnace has an important impact on the control of the resulting surface layers and their properties [8]. So far, numerical simulations of laser and induction hardening [9] and gas jet hardening have been performed [10]. The paper [8] proposes models based on numerical simulation and analytical methods to determine radiation, convection, and heat conduction in heat treatment processes.

The dies are also treated with gas nitriding. The duration of the nitriding process, and thus the thickness of the nitrided layer, is directly correlated with the cost of the process. A die with a worn-out nitrided layer can be re-nitrided [1]. It is possible to find the optimum diffusion layer thickness for which die wear will generate the lowest operating costs [1]. In order to minimise the cost of "regenerating" the dies, the gas nitriding process needs to be precisely controlled. So far, models have been developed for the growth kinetics of the nitrided layer [11]. A weakness of these models is the lack of knowledge of the surface temperature of thermochemically treated components.

Thermochemical treatment processes are used to produce a surface layer of the processed workpiece with improved mechanical properties [12]. Important parameters during the heat treatment processes are the composition and temperature of the gas in the furnace retort, the temperature of the surface to be processed, and the duration of the treatment [11]. The temperature of the furnace atmosphere can be measured with a high level of accuracy. The composition of the furnace atmosphere is regulated and precisely determined throughout the process. During gas nitriding, the surface temperature of the thermochemical workpieces is between ambient and 550°C. In thermal machines, there is a great challenge to determine the precise surface temperature [13, 14]. In thermochemical treatment processes, there is also the problem of determining the precise surface temperature of heat-treated solid components [15, 16]. The direct measurement of the surface temperature of workpieces in atmospheric furnaces is subject to a high error rate [14–16]. In order to precisely determine the boundary condition in terms of temperature, heat flux, or heat transfer coefficient (HTC), the temperature inside the heated element is measured and the inverse problem for the heat conduction equation is solved [17–21]. Inverse problems are numerically determined incorrectly [22–26]. Controlling the heat treatment processes prevents cracking of the work pieces [27]. In the

study [27] the heat treatment of a turbine disc was analysed. Heat transfer coefficients were calculated using the inverse thermal problem. Solving the inverse problem for heat conduction equation was used for the analysis of an incomplete die hardening for aluminium-based foam parts [28].

The inverse model has been used to control of induction heat treatments so far [29]. The temperature in the cylindrical sample was controlled and the nonlinear electromagnetic-thermal problem was solved. In the heat treatment furnace, an inverse problem was used together with an artificial neural network to estimate the optimal control parameters of the heat source [30]. Artificial neural networks together with inverse heat conduction problem were also used to reconstruct the HTC waveform from temperature signals recorded during actual heat treatment processes [31]. The analysis of the heat flow in industrial furnaces in many cases is still based on the operator's experience [8,32]. Heat flow phenomena in furnaces have not yet been adequately studied. A similar issue arises with regard to heat flow in the components being treated.

This paper presents a simulation of the die heating process based on the heat transfer coefficient. This coefficient was determined from the solution of the inverse problem based on experimental data. So far, temperature distributions in thermo-chemically treated dies have not been studied, and the inverse heat conduction problem has not been used to analyze the heating of such components.

2 Description of die geometry and material properties

The paper presents the problem of heating a die for the extrusion of aluminium alloy profiles (Fig. 1). This is a massive component with a complex shape. The temperature changes in selected areas of the die during three heating processes differing in the rate of heating and the intensity of gas flow in the furnace chamber were analysed. The heating processes start at about 295 K (ambient temperature) and finish at about 823 K. The conducted analysis of die heating was performer for gas nitriding. The process starts at ambient temperature and usually reaches the temperature of 823 K. During the heating process, the temperature must correlate with the atmosphere inside the furnace. The proper adjustment of those parameters ensures the creation of surface and near-surface layers with high mechanical parameters. The author heated a roller for chemical and heat treatment

inside the roller at an earlier stage of research also to the temperature of 823 K [16]. The selection of 823 K as the maximum temperature was discussed with individuals responsible for gas nitriding in industrial conditions as well as based on literature [11]. For the temperature range mentioned above, the variation in the heat transfer coefficient and the specific heat is significant. Therefore, the heat flow analyses were performed taking into account the varying properties of WCLV steel as a function of temperature. WCLV steel is tool alloy steel for hot work.

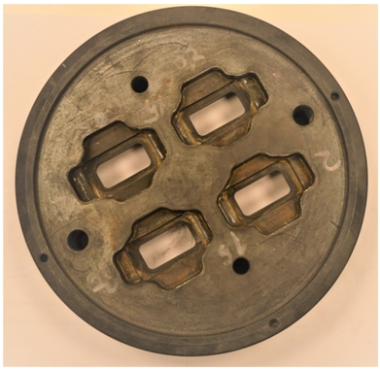

Figure 1: Extrusion die for aluminium alloy profiles [34].

Table 1 presents the chemical composition of the WCLV steel [36]. The temperature dependence of the thermal conductivity and specific heat is shown in Tables 2 and 3 [33]. Linear interpolation was carried out between

Table 1: Chemical composition of the WCLV steel (%) [36]

C	0.35–0.42
Si	0.80–1.20
Mn	0.25–0.50
P	max 0.030
S	max 0.030
Cr	4.80–5.50
Mo	1.20–1.50
W	–
V	0.85–1.15
Co	–
Ni	–

the specified points. Due to the negligible effect of changes in steel density as a function of temperature, the calculation assumes that the steel density does not change and is 7850 kg/m^3 [33].

Table 2: Thermal conductivity coefficient (k) as a function of temperature for WCLV steel

T (K)	k (W/(m K))
293.15	25.5
624.15	27.6
975.15	30.3

Table 3: Specific heat c as a function of temperature for WCLV steel

T (K)	c (J/(kgK))
273.15	460
365.15	521
962.15	620

3 Computational grid

The temperature distribution inside the die was determined using commercial Ansys Transient Thermal software [37]. The calculations were carried out for a three-dimensional model, representing the actual die geometry. Due to the presence of symmetry planes in the die, a quarter of the element was analysed, assuming symmetry conditions in the cross-sectional planes (Fig. 2a, planes marked by green). The mesh constructed from approximately 500 000 tetrahedral elements is shown in Figs. 3 and 4. The impact of the number of mesh elements on the obtained calculation results was analysed. Calculations were also performed for mesh types with higher and lower number of elements than in the case of the selected mesh. Grid elements of three different sizes (G1–G3, Figs. 3 and 4) were used at the main edges of the geometry. The smallest elements of size equal to 5×10^{-4} m (G3, Fig. 4) were used to create a mesh discretization of the edge of the die most mechanically stressed the most during its operation (edge E, Fig. 2b). It is crucial for the correct operation of the die to determine the thermochemical treatment conditions and consequently produce

a layer with high mechanical properties of the mentioned edge. Larger grid elements of 10^{-3} m (G2, Fig. 4) were used to prepare a grid of die sections that do not operate under such harsh conditions as the aforementioned

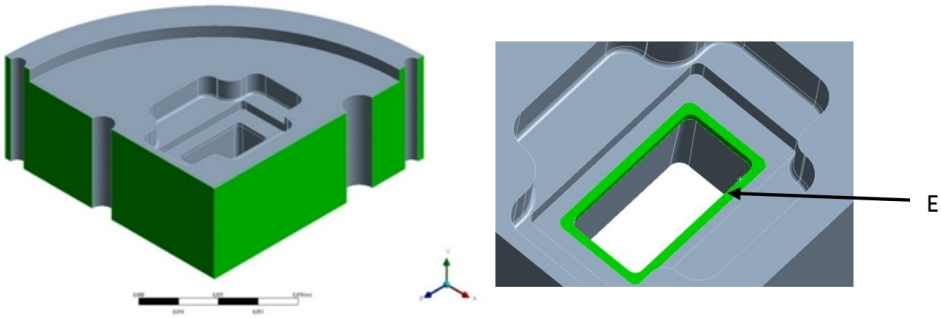

(a) (b)

Figure 2: Fragment of a die with marked: a) planes of symmetry, b) edge E.

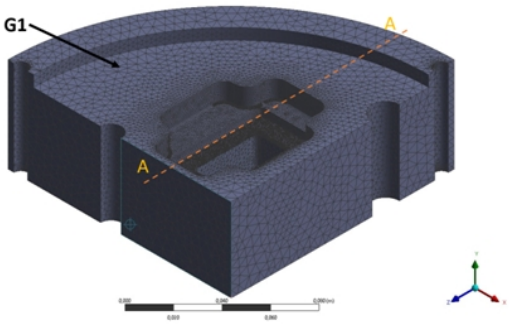

Figure 3: Die fragment mesh with marked G1 type elements.

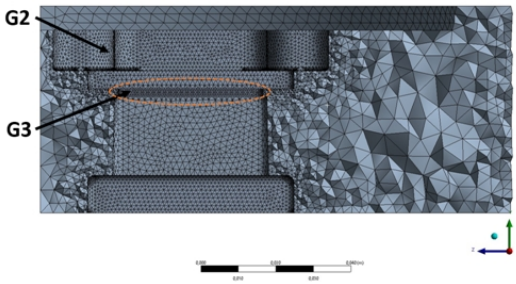

Figure 4: Cross-section $A-A$ of the die grid showing edge E with grid elements G2 and G3 marked.

edge. The grid elements located in other parts of the die were characterised by a grid size of 4×10^{-3} m (G1, Fig. 3). The average orthogonality of the grid elements was 0.75.

4 Initial and boundary conditions

In Ansys Transient Thermal, the heat conduction equation in the die fragment was solved in the following form

$$\rho c(T)\frac{\partial T}{\partial t} = \frac{\partial}{\partial x}\left[k(T)\frac{\partial T}{\partial x}\right] + \frac{\partial}{\partial y}\left[k(T)\frac{\partial T}{\partial y}\right] + \frac{\partial}{\partial z}\left[k(T)\frac{\partial T}{\partial z}\right], \tag{1}$$

where the variability of $k(T)$ is shown in Table 2. The assumed initial die temperature was 295 K. Calculations were carried out using a boundary condition of the form

$$k(T)\frac{\partial T}{\partial n} = h(t)\left[T_g(t) - T_b(t)\right], \tag{2}$$

where $h(t)$ was obtained from solving the inverse problem for the experimental data which are shown in Fig. 6.

Three processes were used to analyse the heating process, differing in the set heating rate and fan speed, which are summarised in Table 4.

Table 4: Heating processes

Process	Heating rate (K/min)	Percentage of maximum fan speed (%)
P1	5	50
P2	5	100
P3	10	50

The heating rate values given in Table 4 are the set values for the furnace control system. Different furnace control modes resulted in different gas temperature waveforms (Fig. 5) and heat transfer coefficient values (Fig. 6) [16, 35]. The boundary conditions in the form of temperature, heat flux and heat transfer coefficient for the cylinder were determined from previous experimental studies in a thermochemical treatment furnace and by solving the inverse problem for the heat conduction equation for the analyzed processes P1–P3 [16]. The inverse heat conduction problem is ill-posed. Even the slightest disturbance in input data can have a significant impact on the calculation results. It was taken into consideration

and self-regulation was done using the time series method described in [16]. The proper selection of a time series significantly reduced the oscillation of the result. A time series of $\Delta t = 30$ s was selected for the analysed processes. So far, on the basis of experimental studies and the stable solution of the inverse heat conduction problem, a slight variation of the heat transfer coefficient at different locations in the furnace working chamber has been shown [15]. Therefore, the boundary condition in the form of the heat transfer coefficient determined earlier in the study was adopted for all the walls of the die model in contact with the furnace atmosphere during the thermochemical treatment. The remaining planes are planes of symmetry (Fig. 2). The boundary conditions obtained from the processes analysed (Table 4) in the form of gas temperature and heat transfer coefficient for the cylinder are shown in Figs. 5 and 6.

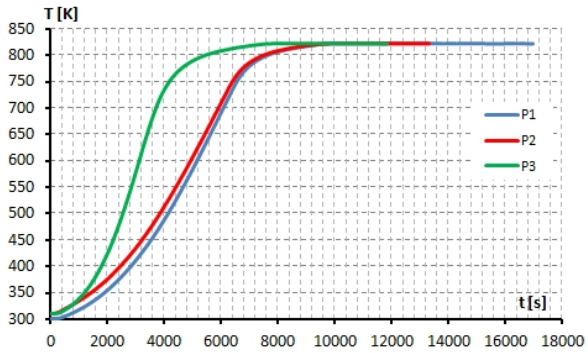

Figure 5: Gas temperature for heating processes P1–P3 in the thermochemical treatment furnace.

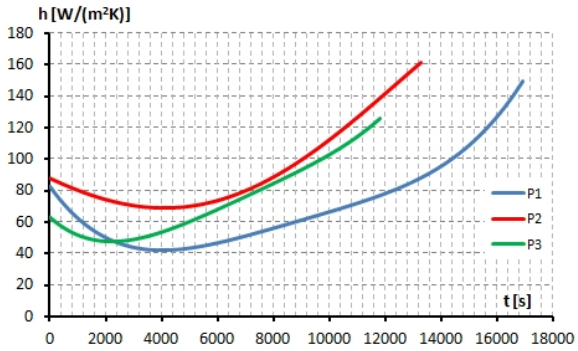

Figure 6: Heat transfer coefficient for heating processes P1–P3 in a thermochemical treatment furnace.

The P1 process had the longest duration and the largest range of heat transfer coefficient values (Fig. 6). At the beginning of the process, the value of h was 84 W/(m^{2}K) after which it decreased to a minimum value equal to 43 W/(m^{2}K) for a time of about 4000 s. Subsequently, the value of the heat transfer coefficient increased and at the end of the process exceeded 140 W/(m^{2}K). The P2 process (Fig. 6) had the same controlled heating rate as the P1 process, but because the fan speed was set to maximum, the gas flow in the furnace chamber was intensified, improving the heat transfer conditions. At the beginning of the process, a higher heat transfer coefficient was obtained than in the P1 process, with a value of 88 W/(m^{2}K). The minimum value for the P2 process is 69 W/(m^{2}K). This occurred for a time of 4100 s. At the end of the process, a heat transfer coefficient value was reached of 160 W/(m^{2}K). The P3 process was characterised by twice the heating rate of the P1 and P2 processes and the fan speed set at 50% of its maximum value. These conditions reduced the process time to 11 820 s. The heat transfer coefficient curves described above were used as boundary conditions in the die heating analysis.

5 Description and analysis of the results for die heating

The effect of the 3D simulation was to obtain the temperature in the entire volume of the die during the heating process. The nature of the gas temperature variation (Fig. 5), the distribution of the heat transfer coefficient (Fig. 6) and the unbalanced distribution of the die mass resulted in uneven heating. The distribution of the difference in the gas temperature and the average die surface temperature for the processes P1–P3 is shown in Fig. 7. This difference reaches 115, 72 and 148 K for processes P1–P3, respectively. Figure 7 shows that the processes examined varied significantly in the values of the temperature difference between the gas and the average temperature of the die surface. The value of the difference is related to the intensity of the heat flow from the gas to the die at the surface. The intensity of heat flow at the surface causes temperature differences in the volume of the die. These, in turn, affect the formation of temperature gradients, thermal stresses and deformations in the die.

Each heating process was characterised by a different distribution of the maximum temperature difference in the volume of the die (Fig. 8). For process P1 and a time of 6540 s, a maximum temperature difference

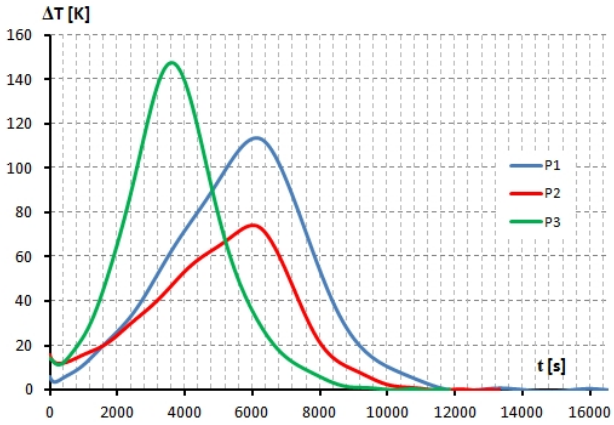

Figure 7: The difference between gas temperature and average die surface temperature during heating for the P1–P3 processes.

in the die volume of 15.2 K was obtained. For the P2 process, a more uniform temperature in the volume of the die was obtained due to the higher value of the heat transfer coefficient. The maximum temperature difference in die volume for the P2 process was 14.2 K. For the P3 process with the highest heating rate, a much larger temperature divergence was obtained in the volume was obtained, which reached a value of 21.2 K for a time of 3780 s. Table 5 summarises the time of occurrence of the maximum temperature divergence values in selected areas: on the heated surface ($T_{\max,A} - T_{\min,A}$), in the volume ($T_{\max,V} - T_{\min,V}$) and on the edge E

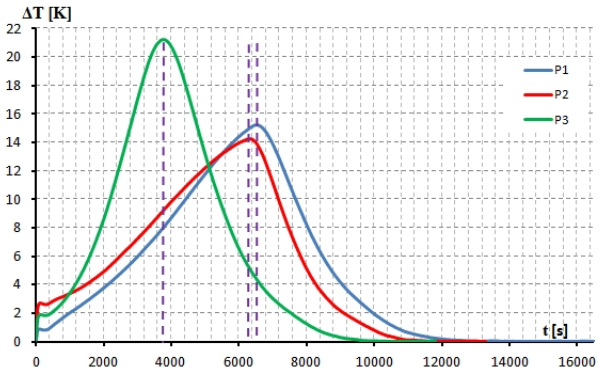

Figure 8: Difference between the maximum and minimum temperatures in the volume of the die.

$(T_{\max,E} - T_{\min,E})$ (Fig. 2b). For each of the analysed heating processes P1–P3, the maximum temperature differences at the edge surface were obtained at the same process time as the maximum differences in die volume.

Table 5: Maximum temperature differences in selected areas of the die and their time of occurrence for each process

Process	t (s)	$T_{\max,A} - T_{\min,A}$ (K)	$T_{\max,V} - T_{\min,V}$ (K)	$T_{\max,E} - T_{\min,E}$ (K)
P1	6540	12.9	15.2	4.2
P2	6390	11.9	14.2	3.9
P3	3780	19.0	21.2	5.9

Figure 9 shows the temperature distribution on the heated die surface according to the boundary condition for the P3 process and the time $t = 3780$ s in which the maximum temperature difference occurred (Table 5). The lowest temperature of about 557 K can be observed in area A with the high mass of the die, while the highest temperature of about 578 K can be observed in area B.

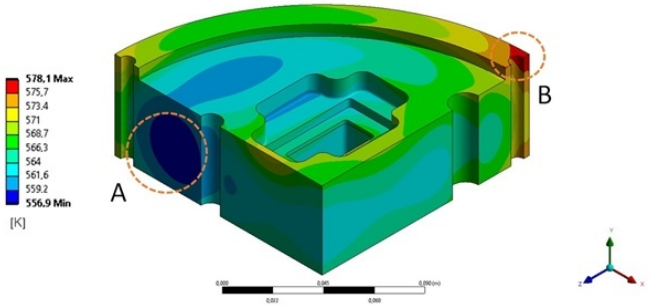

Figure 9: Temperature distribution in the volume of the die in process P3 for time $t = 3780$ s, for which the maximum temperature difference occurred during the entire heating process.

A crucial part of the die geometry is the edge of the die that is mechanically stressed during extrusion of aluminium alloy profiles (the edge E). To give the E-edge the necessary hardness, the die is subjected to gas nitriding. Knowing the exact value of the surface temperature during the process will allow for a precise control of the thermochemical treatment process. For this reason, the temperature distribution on the E edge was subjected to a special analysis. (Figs. 2b, 10, and 11).

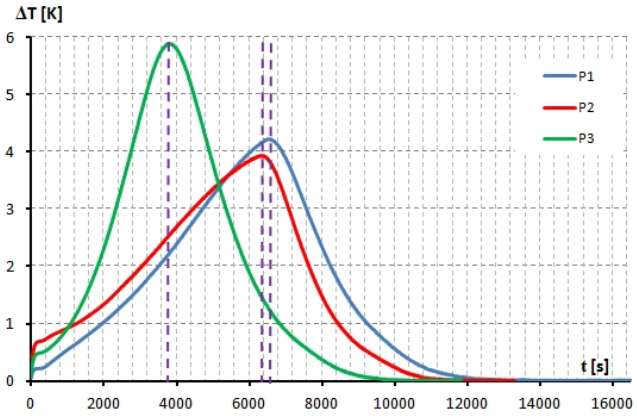

Figure 10: Maximum temperature differences on the surface of the E edge for processes P1–P3.

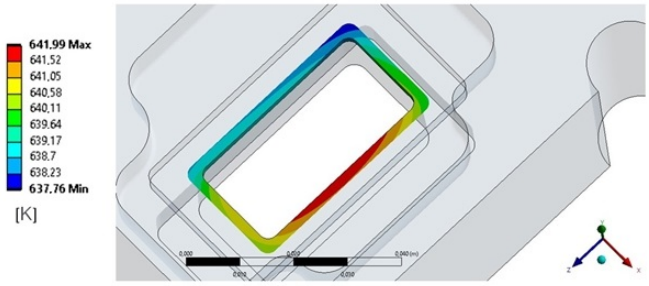

Figure 11: Temperature distribution on edge surface E for process P1 and time $t = 6540$ s.

The maximum temperature difference at the edge surface (Fig. 10) for the analysed processes P1, P2, and P3, respectively, is 4.2, 3.9 and 5.9 K. These are relatively large values considering the precise control of the edge temperature during the nitriding process. Figure 11 shows the temperature field with maximally varying values (for $t = 6540$ s) at the edge surface E for process P1.

For the analysed processes, edge E has the highest temperature on the surface of the long side in the plane of symmetry. For comparison, the lowest temperature occurs at the corner on the side of the high-mass die fragment (area A). The temperature difference then reaches 4.23 K. The temperature distribution at the edge is influenced by the varying mass

of the die geometry. From the analysis of the data obtained for the P1, P2, and P3 process, it can be seen that the position of the maximum and minimum temperature areas does not change for different heating rates and fan settings (gas flow rate in the chamber of the furnace).

6 Conclusions

In the study, the heating of a massive die with complex geometry was analysed. A boundary condition was applied in the form of a heat transfer coefficient obtained for three different heating processes. The variants of boundary conditions considered match the heating rates and fan settings used in thermochemical treatment processes.

The analysis shows that the maximum temperature differences at the edge E occur at the same time as the maximum temperature differences in the volume. The unevenness of the mass distribution of the die is the cause of the temperature variation on the edge E. This variability is significant and reaches 4.2, 3.9, and 5.9 K for P1–P3 processes.

The data show that heating at the maximum fan speed has the positive effect of reducing the process time and achieving a more uniform temperature in the die volume.

In order to achieve a more homogenous temperature in the volume of the component to be worked, and therefore to minimise the occurrence of thermal stresses, it is necessary to intensify: the gas flow in the furnace chamber in order to increase the heat transfer coefficient.

A time-varying heating rate can be used to reduce the temperature differences in the volume of the die. To increase the productivity of the processing, the heating rate can be increased at the beginning and end of each process. However, during the heating stage, when the temperature differences reach a maximum for a constant heating rate, the speed can be reduced. Die heating rate control can be achieved by solving the inverse problem.

Received 9 February 2023

References

[1] Małdziński L., Ostrowska K., Okoniewicz P.: *Controlled ZeroFlow gas nitriding as a method increasing the durability of dies for hot extrusion of aluminum profiles.* Obróbka Plastyczna Metali **25**(2014), 3, 169–183.

[2] Miles N., Evans G., Middleditch A.: *Bearing lengths for extrusion dies: rationale, current practice and requirements for automation.* J. Mater. Process. Tech. 72(1997), 1, 162–176.

[3] Arif A.F. M, Sheikh A.K., Qamar S.Z.: *A study of die failure mechanisms in aluminum extrusion.* J. Mater. Process. Tech. **134**(2003), 3, 318–328.

[4] Fang W., Tang D., Wang H., Li D., Peng Y.: *Optimization of die design for thin-walled flat multi-port tube with the aid of finite element simulation.* J. Mater. Process. Tech. **277**(2020), 116418.

[5] Zinner S., Lenger H., Jesner G., Siller I.: *Analysis of the cooling conditions during heat treatment of die casting dies by use of FEM simulation.* J. Heat Treat. Mater. **67**(2012), 2, 95–99.

[6] Redl C., Friesenbichle, C., Wieser V.: *Numerical simulation of residual stresses during the heat treatment of dies made of hot work tool steel.* Mater. Sci. Forum **524-525**(2006), 433–438. doi: 10.4028/www.scientific.net/MSF.524-525.433

[7] Oliveira M., Duarte A., Coelho P., Marafona J.: *Heat treatment of aluminum extrusion dies and study of their heating by convection/radiation.* Int. J. Adv. Manuf. Technol. **78**(2015), 1–4, 419–430. doi: 10.1007/s00170-014-6618-5

[8] Kang J., Rong Y.: *Modeling and simulation of heat transfer in loaded heat treatment furnaces.* In: Proc. 1st Int. Surface Engineering Cong. – 13th IFHTSE Cong. 7–10 Oct. 2002, 337–343.

[9] Fuhrmann J., Hömberg D.: *Numerical simulation of the surface hardening of steel.* Int. J. Numer. Method. Heat Fluid Fl. **9**(1999), 5–6, 705–724. doi: 10.1108/09615539910286042

[10] Heck U., Fritsching U., Bauckhage K.: *Fluid flow and heat transfer in gas jet quenching of a cylinder.* Int. J. Numer. Method. Heat Fluid Fl. **11**(2001), 1, 36–49. doi: 10.1108/09615530110364079

[11] Małdziński L.: *Thermodynamic, Kinetic and Technological Aspects of Nitrided Layer Production on Iron and Steel in Gas Nitriding Processes.* Wydawnictwo Politechniki Poznańskiej, Poznań 2002 (in Polish).

[12] Dossett J., Totten G.E., Eds.: *ASM Metal Handbook Vol. 4: Steel Heat Treating Fundamentals and Processes.* ASM Int., 1991.

[13] Judt W., Ciupek B., Urbaniak R.: *Numerical study of a heat transfer process in a low power heating boiler equipped with afterburning chamber.* Energy **196**(2020), 117093. doi: 10.1016/j.energy.2020.117093

[14] Taler J.: *Theory and Practice of Identifying Heat Transfer Processes.* Ossolineum, Wrocław – Warszawa – Kraków 1995 (in Polish).

[15] Joachimiak M.: *Analysis of thermodynamic parameter variability in a chamber of a furnace for thermo-chemical treatment.* Energies **14**(2021), 10, 2903. doi: 10.3390/en14102903

[16] Joachimiak M., Joachimiak D., Ciałkowski M., Małdziński L., Okoniewicz P., Ostrowska K.: *Analysis of the heat transfer for processes of the cylinder heating in the heat-treating furnace on the basis of solving the inverse problem.* Int. J. Therm. Sci. **145**(2019), 105985.

[17] Frąckowiak A., Spura D., Gampe U., Ciałkowski M.: *Determination of heat transfer coefficient in a T-shaped cavity by means of solving the inverse heat conduction problem*. Int. J. Numer. Meth. Heat Fluid Fl. **30**(2020), 4, 1725–1742.

[18] Frąckowiak A., Wróblewska A., Ciałkowski M.: *Trefftz numerical functions for solving inverse heat conduction problems*. Int. J. Therm. Sci. **177**(2022), 107566-1-107566-9.

[19] Joachimiak M., Ciałkowski M.: *Optimal choice of integral parameter in a process of solving the inverse problem for heat equation*. Arch. Thermodyn. **35**(2014), 3, 265–280.

[20] Joachimiak M., Ciałkowski M.: *Stable solution to nonstationary inverse heat conduction equation*. Arch. Thermodyn. **39**(2018), 1, 25–37.

[21] Joachimiak M., Joachimiak D., Ciałkowski M.: *Investigation on thermal loads in steady-state conditions with the use of the solution to the inverse problem*. Heat Transfer Eng. **44**(2022), 1–12, 963–969. doi: 10.1080/01457632.2022.2113451

[22] Ciałkowski M., Olejnik A., Joachimiak M., Grysa K., Frąckowiak A.: *Cauchy type nonlinear inverse problem in a two-layer area*. Int. J. Numer. Meth. Heat Fluid Fl. **32**(2022), 1, 313–331.

[23] Joachimiak M.: *Choice of the regularization parameter for the Cauchy problem for the Laplace equation*. Int. J. Numer. Meth. Heat Fluid Fl. **30**(2020), 10, 4475–4492.

[24] Joachimiak M., Ciałkowski M., Frąckowiak A.: *Stable method for solving the Cauchy problem with the use of Chebyshev polynomials*. Int. J. Numer. Meth. Heat Fluid Fl. **30**(2020), 3, 1441–1456.

[25] Joachimiak M., Frąckowiak A., Ciałkowski M.: *Solution of inverse heat conduction equation with the use of Chebyshev polynomials*. Arch. Thermodyn. **37**(2016), 4, 73–88.

[26] Mierzwiczak M., Chen W., Fu Z.-J.: *The singular boundary method for steady-state nonlinear heat conduction problem with temperature-dependent thermal conductivity*. Int. J. Heat Mass Tran. 91(2015), 205–217.

[27] Zhang J., Kang J., Guo Z., Xiong S., Liu B., Zou J., Liu S.: *Study on the heat transfer coefficients during the heat treatment process of a turbine disk*. In: Proc. TMS 2009 138th Ann. Meet. Vol. 2: Materials Characterization, Computation, Modeling, 2009, 27–32.

[28] Lázaro-Nebreda J., Solórzano E., Escudero J., de Saja J.A., Rodríguez-Pérez M.A.: *Applicability of solid solution heat treatments to aluminum foams*. Metals **2**(2012), 4, 508–528. doi: 10.3390/met2040508

[29] Asadzadeh M.Z., Raninger P., Prevedel P., Ecker W., Mücke M.: *Inverse model for the control of induction heat treatments*. Materials (Basel) **12**(2019), 17, 2826. doi: 10.3390/ma12172826

[30] Yadav R., Tripathi S., Asati S., Das M.K.: *A combined neural network and simulated annealing based inverse technique to optimize the heat source control parameters in heat treatment furnaces*. Inverse Probl. Sci. Eng. **28**(2020), 9, 1265–1286. doi: 10.1080/17415977.2020.1719087

[31] Szenasi S., Fried Z., Felde I.: *Training of artificial neural network to solve the inverse heat conduction problem*, In: Proc. 2020 IEEE 18th World Symp. on Applied Machine Intelligence and Informatics (SAMI), Herlany, 2020, 293–298. doi: 10.1109/SAMI48414.2020.9108733

[32] Joachimiak D., Frąckowiak A.: *Experimental and numerical analysis of the gas flow in the axisymmetric radial clearance*. Energies **13**(2020), 21, 5794-1-5794-13. doi: 10.3390/en13215794

[33] Incropera F.P., de Witt D.P.: *Fundamentals of Heat and Mass Transfer*. Wiley, New York 1996.

[34] Photo of a die for the extrusion of aluminium alloy profiles. Poznan University of Technology, Institute of Machines and Motor Vehicles, Poznan 2021.

[35] Joachimiak M., Ciałkowski M.: *Non-linear unsteady inverse boundary problem for heat conduction equation*. Arch. Thermodyn. 38(2017), 2, 81–100.

[36] https://akrostal.pl/stale/wclv-1-2344/?print=pdf (accessed 16 Nov. 2022).

[37] Ansys Transient Thermal Analysis Guide. Ansys 2021R1, Inc.